large range of shifts for the pyrrole resonances within the series Ia–e.

Discussion

The ^1H and ^{13}C NMR data present a self-consistent picture that appears to be in agreement with the current qualitative molecular orbital description[7] of the intermediate-spin (porphinato)iron(III) compounds. Quantum-mechanical admixture involves partial depopulation of the iron $d_{x^2-y^2}$ atomic orbital and π-type unpaired spin delocalization by ligand-to-iron electron transfer from the porphyrin $3e(\pi)$ molecular orbital. The large changes we have induced in the proton and carbon shifts of the perchlorato complexes by varying the phenyl substituents are consistent with changes in occupancy of the $d_{x^2-y^2}$ iron orbital. Much smaller differences are reported (2–3 ppm) for substituent effects on the proton and carbon resonances of low-spin bis(imidazole)(porphinato)iron(III) complexes[13] in which the same $3e(\pi) \rightarrow Fe$ spin-delocalization mechanism is operative but no change in iron orbital occupancy is involved. Therefore, changes in unpaired spin density distribution do not per se produce effects of the magnitude observed for Ia–e. The possibility that the pyrrole proton or carbon shifts result from an equilibrium phenomenon is discounted (for Ia–d) by the upfield progression of the pyrrole β-H resonance with decreasing temperature, which is typical of spin-admixed perchlorato complexes.[7,8]

Upfield proton and carbon shifts are characteristic of $d_{x^2-y^2}$ vacancy[20] and are predicted for an increasing $S = {}^3/_2$ component as $d_{x^2-y^2}$ becomes depopulated. The large upfield shift of the pyrrole proton of $(TPP(2,4,6\text{-}OCH_3))FeClO_4$ suggests that the $d_{x^2-y^2}$ orbital is vacant or nearly so in this complex,[7,20] and hence the complex appears to approach the $S = {}^3/_2$ spin state even at ambient temperature. In addition to the electronic effects of the strongly electron-releasing methoxy substituents, steric hinderance may weaken axial interaction between iron and the perchlorato ligand, causing a further increase in $d_{x^2-y^2}$ orbital energy by producing additional core contraction of the porphyrin.[7]

The observed movement of pyrrole ^1H resonances (Figure 1) toward high-spin shifts with increasingly electron-withdrawing phenyl substituents would result as the decreased repulsive interactions between the $d_{x^2-y^2}$ orbital and the attenuated spin density on the pyrrole nitrogens lower the $d_{x^2-y^2}$ orbital energy and the $d_{x^2-y^2}$ orbital is repopulated. The concomitant downfield shift of the pyrrole carbons is also consistent with behavior expected on repopulating the iron $d_{x^2-y^2}$ orbital with consequent enhancement of unpaired spin delocalization through σ interaction characteristic of the high-spin configuration.[20,21] The relatively constant shift of the meso carbon resonance with changing spin-state admixture reflects small changes in the amount of delocalized unpaired spin density at the meso positions despite variation in spin-state admixture. Changes in unpaired spin density contributed by the high-spin component may be inefficiently transmitted through the σ-framework because of the E-geometric relationship of the meso position to the paramagnetic iron center. The π-delocalization mechanism postulated[7,8] for the intermediate-spin component would be insensitive to the weight of the $S = {}^3/_2$ component in the admixture if the $3e(\pi)$ porphyrin MO, which has a node at the meso carbons, is involved and contact shift makes the predominant contribution to the isotropic shift of the meso carbons. The effect of THF coordination is consistent with stabilization of the $d_{x^2-y^2}$ orbital through axial ligand interaction with iron and the ensuing expansion of the porphyrin core.

Because of crystallite orientation, included solvate, and single-ion anisotropy effects, solid-state magnetic moments cannot be accurately predicted[8] and the values of μ_{eff} determined for the complexes serve primarily to confirm that the properties of Ia–e are consistent with an $S = {}^3/_2, {}^5/_2$ spin state admixture.

Acknowledgment. This work was supported by American Cancer Society Grant BC388.

Registry No. Ia, 91128-43-7; Ib, 57715-43-2; Ic, 92186-38-4; Id, 92186-39-5; Ie, 90764-29-7; $(TPP(4\text{-}OCH_3))FeClO_4{\cdot}2THF$, 92219-73-3.

---

(20) LaMar, G. N.; Walker, F. A. In "The Porphyrins"; Dolphin, D., Ed.; Academic Press: New York, 1978; Vol. IV, p 61 ff.

(21) Goff, H. M. *J. Am. Chem. Soc.* **1981**, *103*, 3714.

Contribution from the Department of Chemistry,
State University of New York at Buffalo, Buffalo, New York 14214

Infrared Study of Ambient-Temperature Chloroaluminates as a Function of Melt Acidity

STEPHEN TAIT and R. A. OSTERYOUNG*

Received January 10, 1984

The infrared spectra of butylpyridinium chloride/aluminum chloride and 1-methyl-3-ethylimidazolium chloride/aluminum chloride room-temperature molten salts have been examined over a range of mole ratios (acidities). Bands observed in the 4000–630-cm^{-1} range have been assigned and spectral changes attributed to the formation of ion pairs, which may involve distortion of the aromatic ring since there is an accompanying loss of aromatic character. This effect is more pronounced in the imidazolium melts where more highly basic melts can be studied due to the greater liquidus range. Several isosbestic points are reported. Addition of H_2O/D_2O to imidazolium melts gave rise to distinct new features in the spectra. In an acidic melt a new spectrum emerged after spectral subtraction, which is believed to be due to the formation of either AlO(OH) or, more likely, $AlOHCl_2$. Addition of H_2O/D_2O to a basic melt gave a complex spectrum.

Introduction

Until recently it has been accepted that melt equilibria in *N*-(1-butyl)pyridinium chloride (BuPyCl)/aluminum chloride ($AlCl_3$) and the 1-methyl-3-ethylimidazolium chloride (ImCl)/aluminum chloride room-temperature melts can be described by the two equilibria[1]

$$AlCl_3 + Cl^- \rightleftarrows AlCl^-$$

$$AlCl_3 + AlCl_4^- \rightleftarrows Al_2Cl_7^-$$

The former is dominant in basic melts, i.e. where the $AlCl_3$:BupyCl mole ratio is less than 1, and the latter in acid melts, where the ratio is greater than 1. The role of the cation had been ignored until Wilkes et al.[2] and Popov[3] undertook

---

(1) Linga, H.; Stojek, Z.; Osteryoung, R. A. *J. Am. Chem. Soc.* **1981**, *103*, 3754.

(2) Fanin, A. A.; King, L. A.; Levisky, J. A.; Wilkes, J. S. *J. Phys. Chem.* **1984**, *23*, 2609.

(3) Taulelle, F.; Popov, A. *Polyhedron* **1983**, *2*, 889.

0020-1669/84/1323-4352$01.50/0

Table I. Spectrometer Settings for Data Collection at 1-cm^{-1} Resolution

Data Collection	
no. of data points/interferogram	16 384
no. of transform points	32 768
no. of data points before center burst	256
high-pass filter (Hz) equivalent to a cutoff at 85 cm^{-1}	100[a]
low-pass filter (kHz) equivalent to a cutoff at 8530 cm^{-1}	10[a]
Scanning Measurements	
no. of scans	1000
precollection beam delay, s	5
total measmnt time, s	1561
scanning time, s	885
mirror velocity, mm of retardation/s	11.72
retardation between points, mm	6.86×10^{-4}

[a] This is the nominal roll-off frequency (3-dB down point) of a Butterworth high/low pass noise filter.

NMR studies of this molten salt system[2,3] and of a similar 1-methyl-3-ethylimidazolium chloride (ImCl) system.[2] Both provided good evidence of ionic interaction (particularly on the basic side), and Wilkes et al. proposed several oligomers to explain the observed behavior.

This problem has not been studied by IR spectroscopy due to the highly corrosive nature of the melts, the lack of resistant, wide transmission windows, and the inability to compensate for the large molten salt absorbances encountered even in short path length cells. The recent acquisition of an FTIR spectrometer and the development of a transmission cell with silicon windows (a configuration thought to possess severe disadvantages)[4,5] has minimized these problems.

In this work the mid-IR spectra of both the BupyCl/$AlCl_3$ and ImCl/$AlCl_3$ melts have been studied as a function of acidity in order to examine the nature of the ionic interaction more closely. Water has also been added to the melt in an attempt to find out more about the "aging" process in melts, and the initial results are reported.

Experimental Section

The experimental details below have been compiled in accordance with the criteria laid down by a subcommittee of the Coblenz Society for the comparison of computerized infrared spectra.[6]

Instrument Information. The spectrometer was manufactured by Nicolet, Model 7199, and was used in unmodified form exclusively for transmission spectroscopy. The detector was a nitrogen-cooled mercury–cadmium–tellurium detector (range 400–5000 cm^{-1}; noise equivalent power 2×10^{-10} WbHz$^{1/2}$). The detector element had an area of 1 mm^2. The source was a water-cooled Globar, and the beam splitter was germanium on a potassium bromide substrate (range 400–4000 cm^{-1}).

Data Collection. A Happ–Genzel apodization function was applied to the double-sided interferogram. The collection parameters used to obtain spectra at a resolution of 1 cm^{-1} are shown in Table I. The times quoted include mirror return and acceleration to constant velocity but not the precollection beam equilibration delay.

Data collection, spectral subtraction, and plotting of spectra were automated with the macro programming system developed in this laboratory.

Sampling Data. The dynamic range of the ADC was 15 bits, and the word length was 20 bits. A system of gain ranging was used in the collection program, which changed the sensitivity away from the center burst of the interferogram to allow detection of small signals.

Spectral Manipulation. For clarity of presentation, smoothing has sometimes been used in spite of the fundamental objection raised by Grasseli et al.[6] that band degradation occurs when data collected on an FTIR are smoothed. Spectra were, however, checked to see that significant absorbance peaks were neither created nor removed by this operation. Values for peak frequency and absorbance were taken from unsmoothed data. An 11-point second-order Savitsky–Golay algorithm was used for smoothing. The absorbance values found after subtraction of the empty cell were corrected for movements of the base line caused by the different refractivities of the filled and empty cell.

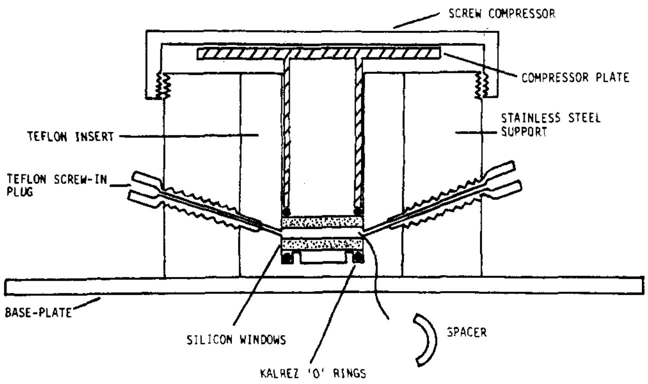

Figure 1. Configuration of IR cell.

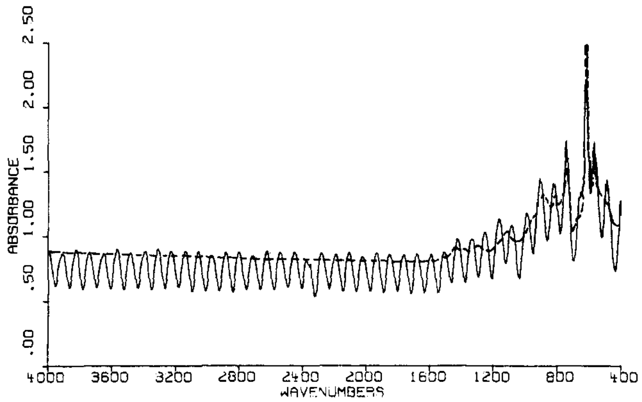

Figure 2. IR spectrum of empty cell with parallel windows (full line) and with tilted windows (dashed line).

No attempt was made to automatically remove water vapor absorbances from spectra. The region near 1650 cm^{-1} containing the sharpest absorbances for this purpose was obscured by absorbances attributable to the melt, and small changes in the background were large relative to the water abosrbance near 3500 cm^{-1}. Since the instrument was kept in an area of controlled low humidity and was continuously purged with nitrogen, this was not a significant problem. Where water or carbon dioxide bands could have led to confusion, the instrument was purged for 15 min before spectra were run.

Sampling Accessories. All sampling accessories were supplied by Harrick Scientific Corp. The cell consisted of a stainless-steel body with a Teflon insert (see Figure 1). The cell windows were 13 mm in diameter and 2 mm in width polished silicon disks and were separated by half-moon spacers of 0.05-mm thickness. The assembly was screwed down to align the cell windows with the entrance and exit to the Teflon plugs. The molten salts flowed through these hollow threaded plugs without contacting the stainless steel.

When the windows were kept parallel by the use of two spacers, five separate lagged interferograms were observed due to reflection, which transformed to give fringes (Figure 2). The unwanted interferograms could be removed in an empty cell by generating a straight line across the sections of the interferogram where the fringes occurred; however, in the presence of melts this led to distortion of the sample spectrum.

When the windows were tilted with respect to each other by using only one spacer (see Figure 3), the lagged interferograms disappeared and a flat base line resulted on transformation (see Figure 2). The cell was maintained in this configuration for all samples; the procedure adopted for filling and emptying the cell is detailed below. The nominal cell path length was 0.025 mm, and the cell volume was 6.3 μL. The

---

(4) Devlin, J.; Li, P.; Cooney, R. "Molten Salts"; Mamantov, G., Ed.; Marcel Dekker: New York, 1969; p 209.

(5) Bandy, A.; Devlin, J.; Burger, R.; McCoy, B. *Rev. Sci. Instrum.* **1964**, *35*, 1206.

(6) Grasseli, J.; Griffiths, P.; Hannah, R. *Appl. Spectrosc.* **1982**, *36* (2), 87.

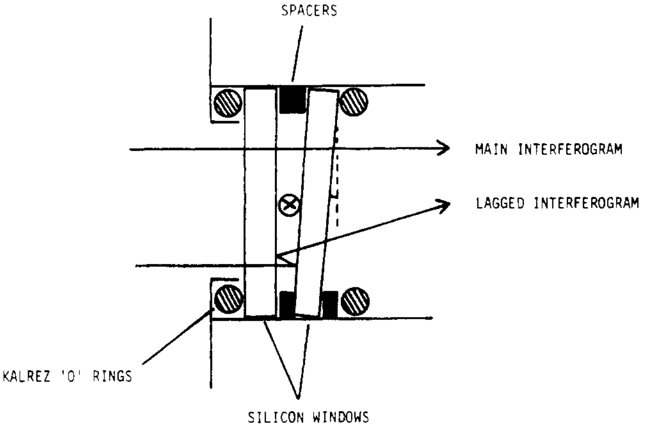

Figure 3. Tilted cell window configuration.

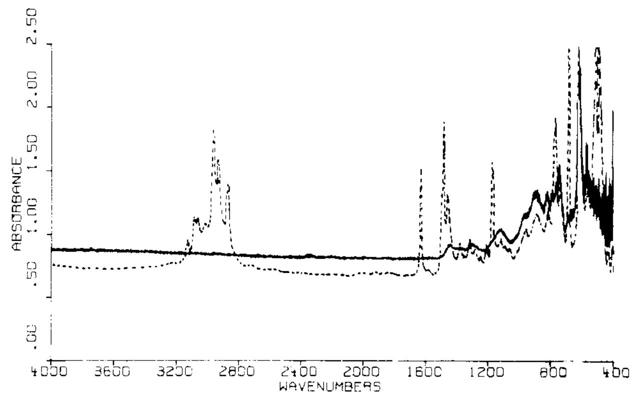

Figure 4. IR spectrum of empty cell (full line) and with 0.8:1 $AlCl_3$/BupyCl melt (dotted line) (unsmoothed data).

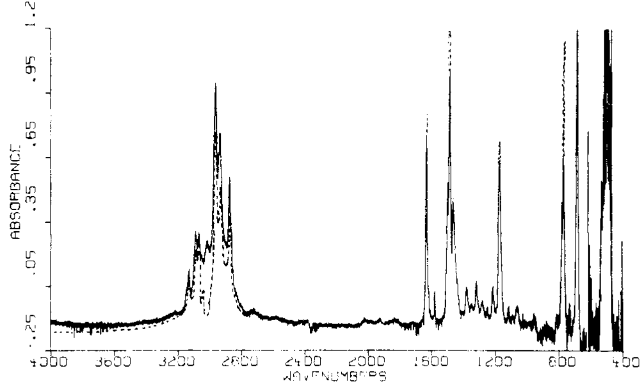

Figure 5. IR spectrum of 0.8:1 (full line) and 2.0:1 (dotted line) $AlCl_3$/BupyCl melts (unsmoothed data).

path length of the cell was checked with the windows parallel using two spacers by measuring the frequency difference between fringes, and the cell path length was found to be accurate to ±5%.

The cell was filled from a 1-mL tuberculin syringe in a Vacuum Atmospheres drybox maintained at <5 ppm of oxygen and water by a Vacuum Atmospheres HE193/2 Dritrain purification system, which circulated the box atmosphere through molecular sieves and a copper catalyst bed to remove oxygen. The cell was angled to avoid trapping bubbles between the opaque silicon windows during filling and sealed with Teflon stoppers. The cell was emptied without diassembly by slowly flushing with 5 mL of methylene chloride to remove the molten salt, 10 mL of methanol to dissolve any residual films, and finally 5 mL of methylene chloride to remove the methanol. The cell was then flushed with argon and dried in vacuo for at least 20 min before being refilled with the next sample.

Chemicals. Anhydrous aluminum chloride (Fluka AG) was distilled once under vacuum in a sealed Pyrex tube from a mixture containing sodium chloride and aluminum wires. This procedure and the preparation of butylpyridinium chloride (BupyCl) has been described elsewhere.[7]

Preparation of 1-methyl-3-ethylimidazolium chloride (ImCl) was based on a method described by Wilkes et al.[8] using a pressure bottle assembly manufactured in our workshop. Following the reaction, a white precipitate formed on cooling and the residual ethyl chloride was vented. Since the product was highly hygroscopic (recrystallization on the open bench resulted in the formation of oils), it was dissolved in hot acetonitrile in a closed glassware apparatus and recrystallized by the addition of cooled ethyl acetate. Seeding assisted recrystallization. After two recrystallizations, the product (mp 82-86 °C) was filtered, dried under vacuum at room temperature, and transferred to the drybox for storage.

Results and Discussion

In previous studies[9] polyethylene had been used as the cell window material for IR work on similar molten salts because of its low background absorbance and inertness to the melt; however, it does absorb strongly in the C–H stretching region (2800–3000 cm^{-1}), and its flexibility makes a fixed path length cell more difficult to obtain. Silicon windows were selected for this work as they appeared to be resistant to corrosion by melts of any acidity, could be arranged to give a reproducible cell path length, and provided a wider transmission window.

The disadvantage of using silicon is its high refractive index, which leads to high background absorbances (~0.75 AU). In addition the spectrum of silicon (607–602 and 626–612 cm^{-1}) and of its impurities (carbon, 607–602 cm^{-1}; oxygen, 1125–1090 cm^{-1}) also interfere;[10] however, since the melt does not interact with the windows, all but the major silicon absorbance at 620 cm^{-1} (i.e., absorbances less than 2 AU) can be subtracted without any alteration to the sample spectrum. Where the absorbance exceeds 2 AU (i.e., less than 1% transmission), subtraction becomes less accurate and the result is a confused differential. This work has, therefore, been restricted to the 4000–630-cm^{-1} range.

Melt spectra were recorded over a range of acidity from 0.8:1 to 2:1 $AlCl_3$/BupyCl and from 0.4:1 to 1.75:1 $AlCl_3$/ImCl. In order to compare melts of different acidity, the spectra were corrected for cation dilution by multiplying the spectra by a correction factor after the background cell window spectrum had been subtracted. The molar cation concentration is given by

$$[R^+] = \frac{(\text{mole fraction of RCl})(\text{density} \times 10^3)}{\text{binary mol wt}}$$

where R^+ = butylpyridinium or imidazolium cation, and the binary molecular weight is given by

$$\text{binary mol wt} = [(\text{mol fraction of } AlCl_3)(\text{mol wt of } AlCl_3) + (\text{mole fraction of RCl})(\text{mol wt of RCl})]$$

The correction factor is the ratio of the cation concentration in a particular melt to the cation concentration in a 0.8:1 $AlCl_3$/BupyCl for BupyCl melts or in a 0.4:1 $AlCl_3$/ImCl for ImCl melts (see Table II).[11] Thus, any absorbances unaltered by changes in melt acidity after correction are inferred to be due to vibrations that are not affected by melt interactions.

IR Spectra. $AlCl_3$/BupyCl Melts. The IR spectra of an empty cell alone and one filled with 0.8:1 $AlCl_3$/BupyCl melt

---

(7) Robinson, J.; Osteryoung, R. A. *J. Am. Chem. Soc.* **1979**, *101*, 323.
(8) Wilkes, J.; Levisky, J.; Wilson, J.; Hussey, G. *Inorg. Chem.* **1982**, *21*, 1263.
(9) Gale, R.; Osteryoung, R. A. *Inorg. Chem.* **1980**, *19*, 2240.
(10) Vidrine, W. *Anal. Chem.* **1980**, *52*, 92.
(11) Fannin, A.; King, L.; Stech, D.; Vaughn, R.; Wilkes, J.; Williams, J. Proceedings of the Symposium on Transport Processes in Electrochemical Systems, The Electrochemical Society, Montreal, 1982; in press.

Table II. Cation Concentration Correction Factors for the Normalization of BupyCl and ImCl Melt Spectra

Imidazolium Chloride/Aluminum Chloride Melts

mole ratio of $AlCl_3$/ImCl	melt density,[a] g/cm^{-3}	mole fraction of ImCl	binary melt mol wt	cation concn, mol/L	corrn factor
0.4	1.21	0.71	142.8	6.02	1.0
0.55	1.23	0.65	142.0	5.63	1.07
0.7	1.25	0.59	141.1	5.22	1.15
0.85	1.27	0.54	140.5	4.88	1.23
0.95	1.28	0.51	140.1	4.66	1.29
1.0	1.28	0.50	140.0	4.57	1.32
1.25	1.31	0.44	139.2	4.22	1.43
1.5	1.34	0.40	138.7	3.87	1.56
1.75	1.35	0.36	138.1	3.52	1.71
2.0	1.38	0.33	137.7	3.31	1.82

Butylpyridinium Chloride/Aluminum Chloride Melts

mole ratio of $AlCl_3$/BupyCl	melt density, g/cm^{-1}	mole fraction of BupyCl	binary melt mol wt	cation concn, mol/L	corrn factor
0.8	1.22	0.56	154.8	4.41	1.0
0.85	1.23	0.54	154.0	4.31	1.02
0.9	1.23	0.53	153.6	4.24	1.04
0.95	1.24	0.51	153.0	4.13	1.07
1.25	1.28	0.44	150.2	3.75	1.17
1.5	1.30	0.40	148.7	3.50	1.26
1.75	1.32	0.36	147.1	3.23	1.36
2.0	1.33	0.33	146.0	3.00	1.47

[a] Extrapolated or interpolated from data by Wilkes et al.[11]

are shown in Figure 4. The subtraction of these two spectra and a similar subtraction for a 1.8:1 $AlCl_3$/BupyCl melt are shown in Figure 5. The peak frequencies and absorbances of the two melts are detailed in Table III and compared with the same data for the methylpyridinium cation.[12]

As expected, there are both similarities and differences, most of the latter attributable to the presence of the butyl group. There is increased aliphatic C–H stretching (2850–3000 cm^{-1}), C–H/C–N mixed out-of-plane bending modes (1347–1454 cm^{-1}), C–N stretching (1251 cm^{-1}), aromatic C–H in-plane bending (950-1230 cm^{-1}), and C–H bending (686 cm^{-1}). The last band only occurs strongly where there are at least four adjacent methylene groups in the alkyl chain.[13]

The spectra of acidic and basic melts were very similar. Many of the bands were sharp in the acidic melt but broader in the basic melt (e.g., 1214, 1320, 1464–1501, 1584, 1634 cm^{-1}), and peak frequencies were lower by between 2 and 6 cm^{-1}. Both the loss of symmetry suggested by the first effect and the peak shift are indicative of an interaction, perhaps ion-pair formation, though the magnitude suggests that this is not a strong effect. Similar and more pronounced effects are observed in the ImCl/$AlCl_3$ melts (see below) where studies could be performed in more basic melts.

The absorbance change in intensity[9] at 1450–1500 cm^{-1} in acidic melts found by Gale and Osteryoung was observed, but the bands at 1256 and 1360 cm^{-1} could not be reproduced. This may indicate that polyethylene windows employed in this earlier study were not inert to attack by acidic melts.

The main difference between acidic and basic melts was in the C–H stretching region. A new broad band emerged at 3018 cm^{-1} as the melt was made basic (see Figure 6). A similar band appears in the ImCl melts (see below), but the source of this band is not known.

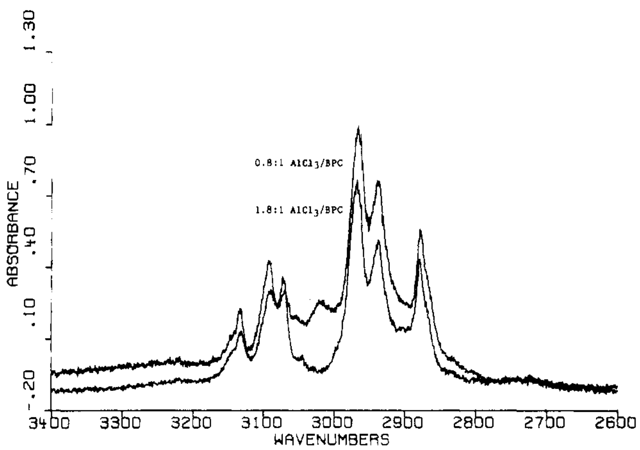

Figure 6. IR spectrum of 0.8:1 and 1.8:1 $AlCl_3$/BupyCl melts (unsmoothed data).

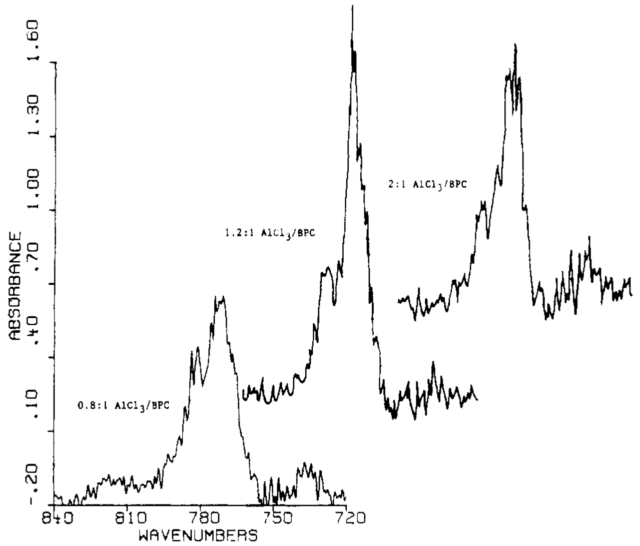

Figure 7. IR spectrum of 0.8:1, 1.2:1, and 2:1 $AlCl_3$/BupyCl melts (unsmoothed data).

In spite of the interference caused by this effect, it appears that the intensities in the aliphatic C–H stretching region at 2970–2870 cm^{-1} are enhanced and that the intensities of C–H aromatic bands at 3130–3070 cm^{-1} are diminished as the acidity decreases. These changes indicate a loss in ring aromaticity, which has also been observed by NMR where proton chemical shifts tend toward those expected of a conjugated alkene as melts are made more basic.[2,14]

Further differences arise in the 660–840-cm^{-1} region (see Figure 7). A multipeaked band was observed at 773 cm^{-1} in a 1.2:1 $AlCl_3$/BupyCl melt with a shoulder at 782 cm^{-1}. The area of the band decreased with increasing acidity or basicity from a neutral melt (spectra could not be obtained in the neutral region itself as the melt solidified at room temperature). The band shape also distinctly altered, and the peak altered to 772 cm^{-1} in 0.8:1 $AlCl_3$/BupyCl and 768 cm^{-1} in 2:1 $AlCl_3$/BupyCl melt. The shoulder at 782 cm^{-1} remained unaltered.

A large off-scale absorbance at 670–695 cm^{-1} varied in intensity in the same way but was only on-scale in the 2:1 $AlCl_3$/BupyCl melt. The band consisted of a broad absorbance at 691 cm^{-1} with two peaks superimposed on it at 686 and 683 cm^{-1}. The absorption bands in this region were, however, very large.

---

(12) Spinner, E. *Aust. J. Chem.* **1967**, *20*, 1805.

(13) Bellamy, L. "The Infrared Spectra of Complex Molecules"; Chapman and Hall: London, 1975; p 29.

(14) Sykes, P. "A Guidebook to Mechanisms in Organic Chemistry", 4th ed.; Richard Clay Ltd.: London, 1965; p 18.

Table III. Comparison of the IR Spectra of 0.8:1 and 1.8:1 $AlCl_3$/BupyCl Melts with That of Methylpyridinium Iodide

	methylpyridinium iodide cryst		0.8:1 $AlCl_3$/BupyCl melt		1.8:1 $AlCl_3$/BupyCl melt	
band assgnt[a]	peak freq[b]	abs[c]	peak freq	abs	peak freq	abs
	3134	0.1	3134	0.41	3132	0.27
	3118	0.1	3121	0.32		
Ar C-H str	3081	0.05	3090	0.58	3091	0.47
ar C-H str/b	3074	0.25	3078	0.54		
	3056	0.1	3054	0.43	3048	0.08
Ar C-H stry asym	3038	0.45				
N-H str assn			3018	0.31		
Me C-H str asym	2990	0.15				
Me C-H str sym	2967	0.05	2967	1.15	2968	0.81
aliphatic C-H str			2940	0.91	2938	0.57
aliphatic C-H str			2906	0.52		
aliphatic C-H str			2878	0.78	2879	0.49
aliphatic C-H str			2870	0.64	2870	0.30
aromatic C-C str	1632	0.8	1634	0.87	1634	1.01
aromatic C-C str	1581	0.15	1583	0.22	1584	0.16
aromatic str/deformn	1501	0.8	1501	0.70	1501	0.78
aromatic str/deformn	1486	0.9	1488	1.14	1489	1.42
comb 681/783			1464	0.70	1466	0.60
Me C-H asym b	1444	0.1	1444	0.38		
Me C-H asym b	1419	0.05				
			1384	0.33	1384	0.21
Me C-H sym b	1347	0.01	1350	0.25	1352	0.14
ring b i/p sym	1318	0.03	1320	0.38	1320	0.24
ring b i/p sym	1287	0.3	1285	0.30	1285	0.14
ring b i/p sym	1224	0.15	1251	0.24	1251	0.10
ring b i/p sym	1210	0.3	1214	0.35	1214	0.18
ring b i/p asym	1189	0.7	1175	0.77	1176	0.89
	1150	0.15				
C-H b i/p	1135	0.25	1118	0.23	1118	0.20
C-H b i/p	1057	0.20	1064	0.24	1064	0.17
i/p str asym	1025	0.1	1029	0.18	1029	0.09
ring b o/p	954	0.1	955	0.20	956	0.18
ring b o/p asym	868	0.05				
ring b i/p asym	800	0.02			818	0.16
Me C-H b ?			783	0.55	781	0.55
ring b o/p asym	773	0.70	772	1.14	768	1.31
ring b o/p asym	771	0.79				
			738	0.21	735	0.24
ring b o/p sym	678	0.9				
CH_2 b			686	4.0	681-686	4.0

[a] Abbreviations for this and the following tables: str, stretching; b, bending; deformn, deformation; i/p, in plane; o/p, out of plane; sym, symmetrical; asym, asymmetrical; assn, association. [b] Frequencies in cm^{-1}. [c] Absorbance values have been corrected for nonzero base line error arising out of the difference in refractive index of the cell empty and filled with melt.

The vibrational modes of pyridine assigned by Spinner[12] were based on the degenerate vibrational modes of benzene described by Lord et al.[15] The aromatic out-of-plane modes are assigned to the 772- and 683-cm^{-1} bands.

Association by the cation with species above or below the plane of the molecule (i.e., ion pairing) might reduce the intensity of the vibration. The 683-cm^{-1} band is more affected than the 772-cm^{-1} band. This postulated association is consistent with the observation of Wilkes et al.[2] in NMR studies on these molten salts.

In summary, the change in band shape and intensity as the melt acidity is varied across the range suggests that intermolecular interaction, perhaps ion-pair formation, is taking place in both the acidic and basic melts. Loss of aromaticity in the basic melts suggests that there may be some ring distortion associated with this interaction.

$AlCl_3$/ImCl Melts. Infrared spectra for the 0.4:1 $AlCl_3$/ImCl and 1.5:1 $AlCl_3$/ImCl melts with silicon cell window absorbance subtracted are shown in Figure 8. The peak frequencies and absorbances for these two melts and for ImCl in methylene chloride are tabulated and assigned in Table IV. The same data for liquid imidazole are also included to differentiate bands that could be attributable to either the organic cation or inorganic species. The spectra have all been corrected for changes in cation concentration as before (see Table II).

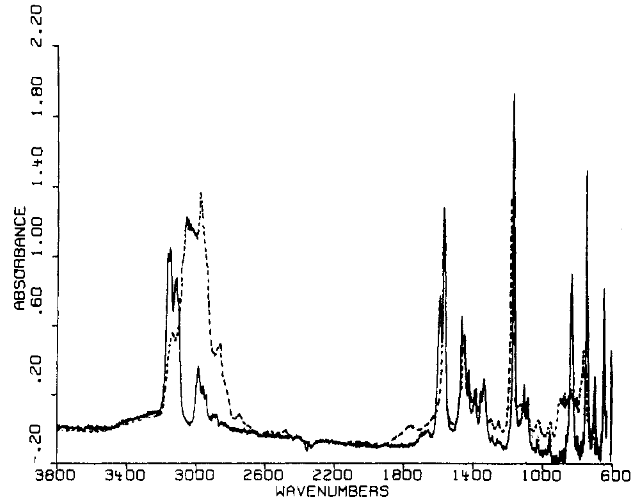

Figure 8. IR spectrum of 0.4:1 (dotted line) and 1.5:1 (full line) $AlCl_3$/ImCl melts (unsmoothed data).

Imidazole has been the subject of several IR studies,[16],[17]

---

(15) Lord, R.; Marston, A.; Miller, F. *Spectrochim. Acta* **1957**, *9*, 113.

Table IV. Comparison of the IR Spectra of 0.4:1 and 1.5:1 $AlCl_3$/ImCl Melts (0.5 M in Methylene Chloride and Liquid Imidazole)

	0.4:1 $AlCl_3$/ImCl melt		1.5:1 $AlCl_3$/ImCl melt		0.5 M ImCl in CH_2Cl_2		imidazole[19]
band assgnt	peak freq[a]	abs	peak freq	abs	peak freq	abs	peak freq
aromatic C-H str	3148	0.57	3167	1.0	3145	0.1	
aromatic C-H str			3122	0.87			3124
			3100	0.73			3105
N-H/O-H assn					3074	0.18	
N-H/O-H assn	3052	1.22			3039	0.30	3021
N-H/O-H assn	3018	1.20					
aliphatic C-H str			2993	0.36	2999	0.25	
aliphatic C-H str	2982	1.38	2963	0.25			
aliphatic C-H str			2943	0.20	2956	0.42	
N-H ?	2866	0.48			2865	0.14	
HCl ?	2833	0.28					
N-H ?	2749	0.09			2730	0.04	2800
HCl ?	2677	0.02					2587
N-H assn	1764	0.13			1732	0.05	
comb			1678	0.10			
C-C=N$^+$-			1594	0.90			
comb					1587	0.09	1573
ring str sym	1569	1.22	1569	1.42	1573	0.22	1541
ring str sym	1464	0.60	1469	0.80	1467	0.11	1490
ring str sym	1458	0.60	1454	0.68	1454	0.09	1450
Me C-H b assym	1427	0.38	1428	0.51	1428	0.08	
Me C-H b assym	1389	0.35	1390	0.39	1388	0.08	
ring str sym	1355	0.32	1357	0.39	1358	0.07	1323
Me C-H b sym	1344	0.32	1344	0.41	1343	0.09	
ring str sym	1336	0.44	1336	0.42	1337	0.09	
ring C-H b sym	1302	0.20	1292	0.13	1302		1260
N-H i/p b	1252	0.17	1246	0.16			1242
ring str sym	1179	1.50	1167	2.54	1178	0.37	1140
ring C-H i/p b	1108	0.22	1108	0.50			1099
ring C-H i/p b	1080	0.31	1090	0.35			1052
comb							972
comb	1027-1033	0.17			1037	0.07	
N-H i/p b/C-H i/p b	959	0.16	959	0.14	959	0.02	934
ring i/p b					896	0.08	894
C-H i/p b			834	1.13			835, 827
	794-899	0.29					
ring o/p b asym							756, 736
ring o/p b asym	761	0.35	749	1.22	750	[b]	
Al-O str	704	0.09	703	0.3		[b]	
ring b as	651	0.53	645	0.85	650	[b]	657
ring b as	617-631	>8.0[c]	618-630	>8.0[c]		[b]	619

[a] Frequencies in cm^{-1}. [b] Obscured by C-Cl stretching absorbance. [c] Combined with Si cell window absorbance.

Table V. Comparison of Peak Frequency (cm^{-1}) and Intensity Changes Occurring with Melt Acidity

	aromatic C-H str		aliphatic C-H str		-C=N- str		ring str		ring i/p b		ring o/p b	
mole ratio $AlCl_3$/ImCl	peak freq	abs	peak freq	abs	peak freq	abs	peak freq	abs	peak freq	abs	peak freq	abs
0.40:1	3148	0.63	2981	1.43	1590	0.29	1178	1.48	834	0.34	760	0.46
0.55:1	3154	0.73	2983	1.25	1590	0.38	1175	1.44	838	0.45	758	0.60
0.70:1	3156	0.85	2985	1.05	1591	0.48	1172	1.55	837	0.58	754	0.84
0.85:1	3157	0.90	2987	0.76	1592	0.64	1170	1.98	837	0.76	751	1.04
0.95:1	3158	1.08	2988	0.52	1592	0.67	1168	1.57	837	0.95	747	1.05
1.0:1	3159	1.02	2990	0.40	1595	0.72	1170	1.87	838	1.19	747	1.20
1.20:1	3159	0.98	2991	0.40	1595	0.71	1169	2.15	837	1.09	747	1.30
1.50:1	3161	1.00	2992	0.39	1595	0.78	1169	2.14	836	0.98	747	1.42
1.75:1	3161	1.03	2993	0.40	1595	0.85	1169	2.46	835	1.08	747	1.62
peak shift between 0.4:1 and 1.0:1 melts	−11		−9		5		8		4		13	
peak shift between 2.0:1 and 1.0:1 melts	2		3		0		1		3		0	

and the spectrum is complicated by coupled vibrations arising from the heterocyclic ring and by considerable N-H···N association effects. In addition, the positions of bands are known to move when the ring positions are substituted[18] though 1,3-substitution removes N-H association.

In general, many of the bands found in the melt are in a position similar to those found in imidazole, but shifted to lower frequencies due to the inductive effect of the alkyl groups. Bonds have been assigned on the basis of peak position, intensity, and sensitivity to ring substitution relative to imidazole and its derivatives.[19] The spectrum of ImCl in methylene chloride is very similar to that of the 0.4:1 $AlCl_3$/ImCl basic melt but is different in acidic melts, which suggests interaction,

---

(16) Bellocq, A.; Perchard, C.; Novak, A.; Josien, M. *J. Chem. Phys.* **1965**, *62*, 1334. Perchard, C.; Novak, A. *Ibid.* **1968**, *48*, 3079.
(17) Hodgson, J.; Percy, C.; Thornton, D. *J. Mol. Struct.* **1980**, *66*, 81.
(18) Pouchert, C. "The Aldrich Library of IR Spectra", 3rd ed.; Aldrich Chemical Co.: Milwaukee, WI, 1981; p 1195.
(19) Cordes, M.; Walter, J. *Spectrochim. Acta, Part A* **1968**, *24A* 237.

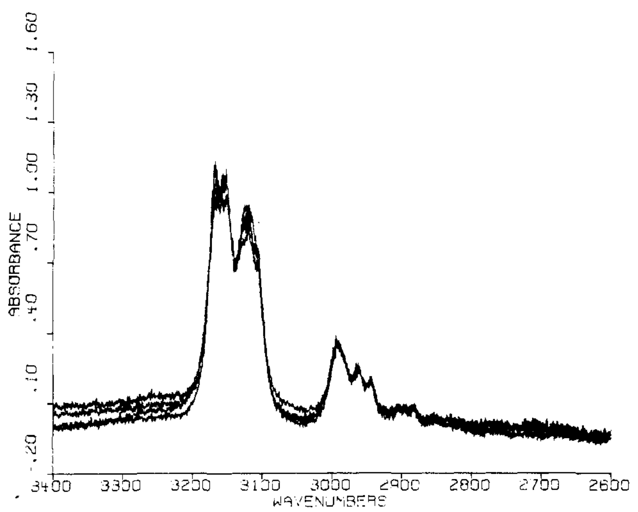

Figure 9. Superimposition of 1:1, 1.2:1, 1.5:1, and 1.75:1 $AlCl_3$/ImCl melts (11-point data smoothing).

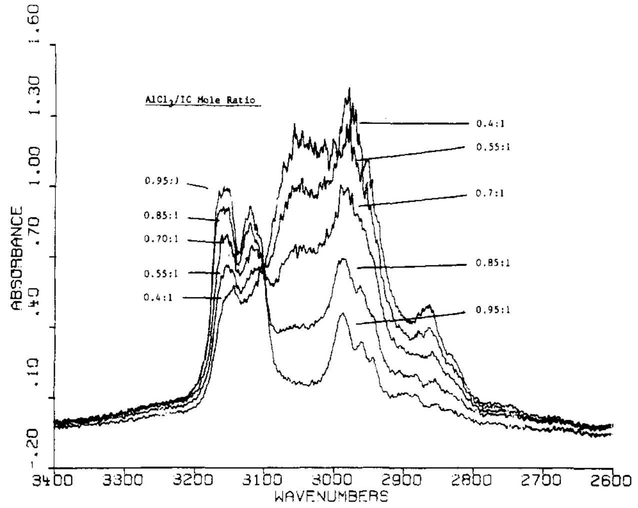

Figure 10. IR spectrum of 0.4:1, 0.55:1, 0.7:1, 0.85:1, and 0.95:1 $AlCl_3$/ImCl melts (11-point data smoothing).

perhaps the formation of ion pairs, in both methylene chloride and the basic melt. The broadening and shift of peaks observed in the BupyCl melts occurred more strongly in the ImCl melts; the change in peak frequency and absorbance of the most sensitive bands are tabulated in Table V. The changes in the basic melts were more marked than for BupyCl since more basic melts are attainable, but there were only small alteration to the spectra over the acidic range. Thus, specific interactions, perhaps ion-pair formation, appear to be much stronger in the basic than in the acidic melt.

Differences between the acid and basic melts can be split into three regions: 3600–1600, 1600–900, and 900–630 cm^{-1}.

Region 1: **3600–1600 cm^{-1}.** Virtually no change was observed as the melt acidity was altered from 2:1 to 1:1 $AlCl_3$/ImCl, and the resulting spectra were almost superimposable after correction for concentration changes (see Figure 9); thus, Beer's law was obeyed for these melts down to at least 1% transmission, a fact that is most important in considering the changes taking place in the basic melts.

In the basic region there were considerable changes as the melt acidity was varied from 0.4:1 to 1:1 $AlCl_3$/ImCl (see Figure 10). A broad band with peaks at 3052 and 3018 cm^{-1} increased as the melt was made more basic and distorted the other bands in this region. The aromatic band at 3167 cm^{-1} diminished considerably, and the band at 3114 cm^{-1} nearly disappeared under the 3052/3018-cm^{-1} band. An isosbestic point occurs at 3103 cm^{-1}, indicating an interaction involving at least two species whose concentrations vary with acidity. The aliphatic C–H stretching band at 2993 cm^{-1} shifts to 2982 cm^{-1}, and the bands at 2963 and 2943 cm^{-1} behaved similarly, becoming indistinguishable from the broad bands at 3052/3018 cm^{-1} in very basic melts.

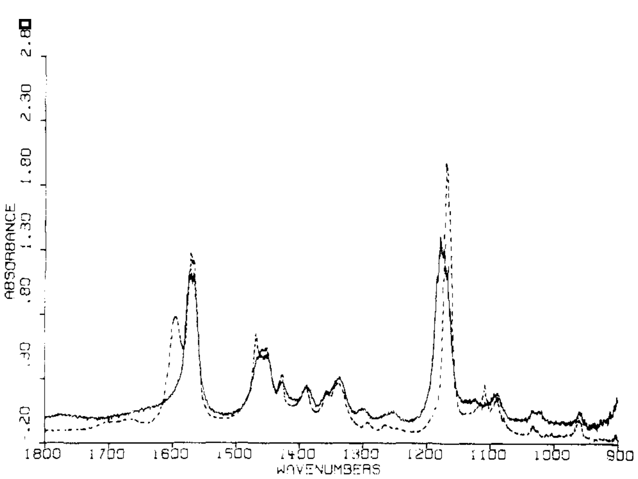

Figure 11. IR spectrum of 0.4:1 (solid line) and 1.5:1 (dashed line) $AlCl_3$/ImCl melts (unsmoothed data).

As with the BupyCl melt, the broad band at 3052/3018 cm^{-1} varies with melt acidity in the basic region. Bands in a similar region have been studied in liquid imidazole by Bellocq et al.[16] who attributed them to a hydrogen bond, HN--H association. They deuterated imidazole in the 1-position and shifted the part of this region responsible for this effect. The band position (assuming a value of ν_{N-H}/ν_{N-D} of 1.34), shape, and intensity are similar to that seen in this melt. While recent studies support the explanation of Bellocq et al. on the breadth and complexity of the bands in this region observed in imidazole,[19,20] the presence of the band in the ImCl melt, however, should not be due to similar interaction, since both of the nitrogen atoms are substituted, but there is no obvious source of available proton, except for perhaps traces of water, in the melt. This band could possibly be due to a hydrogen-bond type of interaction between Cl$^-$ and H on C-2 of the imidazole ring. (Note that a band in a similar region varies with acidity in the BupyCl melt.) In acid melts this broad band is absent, and in the basic melts its intensity is clearly a direct function of the chloride concentration. Since this band also occurs in the basic BupyCl melts, it is not a function of the imidazole ring but could be related to an aromatic-ring nitrogen or, as mentioned above, to a hydrogen bond between chloride and hydrogen in the butylpyridinium or imidazolium cation.

A broad low-intensity absorbance in the 2600–2900-cm^{-1} region in the neutral and acidic melts becomes enlarged in the basic region, and peaks emerged at 2866, 2833 (sh), 2750, and 2677 cm^{-1}.

In the 2600–1600-cm^{-1} region the absorbances are small and have been assigned previously to nonfundamental modes, i.e. overtones or combination bands.[19] The absorbance found at 1765 cm^{-1} in 0.4:1 $AlCl_3$/ImCl is absent in acidic melts. The band at 1660–1680 cm^{-1}, which is bserved in the 1.5:1 $AlCl_3$/ImCl melt but obscured in the 0.4:1 $AlCl_3$/ImCl melt is probably due to either an overtone of the 834-cm^{-1} band and/or combination of the 1033- and 645-cm^{-1} bands.

Region 2: **1600–900 cm^{-1}.** In addition to the general broadening and shifting of peaks already mentioned, a shoulder on the 1570-cm^{-1} peak emerges at 1590 cm^{-1} (see Figure 11). This enlarges to a separate peak at 1595 cm^{-1} in acidic melts

---

(20) Majoube, M. *J. Mol. Struct.* **1980**, *61*, 137.

Scheme I

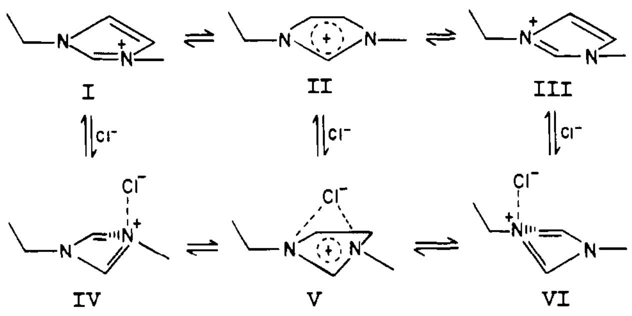

and cannot be attributed to a combination band. The change in peak frequency and intensity is shown in Table V.

Similar effects have been recognized in studies of α,β-unsaturated tertiary amines,[21,22] where increases of peak frequency of 20–50 cm^{-1} have been observed on going from an α,β-unsaturated amine (enamine) to its perchlorate salt corresponding to the transformation

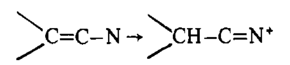

$$>C=C-N \rightarrow >CH-C=N^+$$

For instance, 1-*n*-butyl-2-methyltetrahydropyridine absorbs at 1649 cm^{-1} in the base form and 1684 cm^{-1} as the perchlorate salt. For aromatic rings this structural change amounts to a loss of aromaticity and characteristics more similar to a conjugated tertiary amine. In the melts the shift between the acidic melt and the 1570-cm^{-1} peak is 25 cm^{-1}; thus, it appears that the I or III forms of the cation (see Scheme I) have more significance as the chloride concentration is increased.

Region 3: 900–630 cm^{-1}. As for the BupyCl melts the ring bending modes of vibration are the most sensitive to changes in melt acidity (Figure 12). The in-plane ring bending band at 834 cm^{-1} diminishes with little change in peak frequency as the acidity is reduced and is replaced by a very broad band (794–899 cm^{-1}) in highly basic melts. Isosbestic points are observed at 823 and 853 cm^{-1} as this change takes place. Subtraction in this region is less accurate than in higher wavenumber regions.

The out-of-plane bending mode at 760 cm^{-1} shifts to higher frequencies and broadens significantly (see Table V). The two modes of vibration are[19]

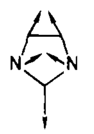

in-plane ring bending at 834 cm^{-1}

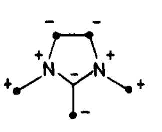

out-of-plane C—H bending at 760 cm^{-1}

and it again appears that modes of vibration that distort the position of the ring nitrogen atoms are more sensitive to acidity changes. When this observation is linked with the enamine effect, the loss of aromaticity, and the electronic repulsion between the chloride ion and the π electrons of the ring, distortion of the ring is suggested. This is illustrated in Scheme I.

Wilkes et al.[2] have suggested on the basis of their NMR studies that ion interactions occur in the form of oligomeric chains held together by ion–ion interactions in the basic melts.

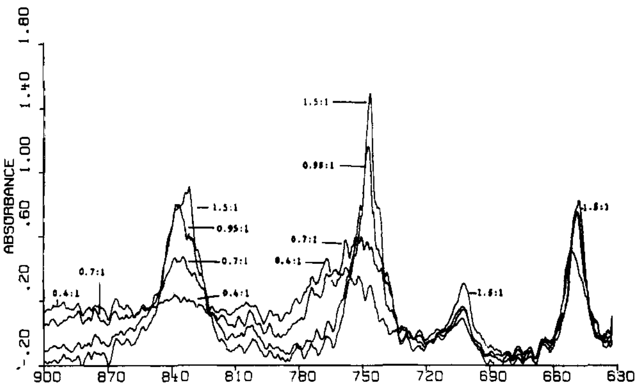

Figure 12. IR spectrum of 0.4:1, 0.70:1, 0.95:1, and 1.5:1 $AlCl_3$/ImCl melts (11-point data smoothing).

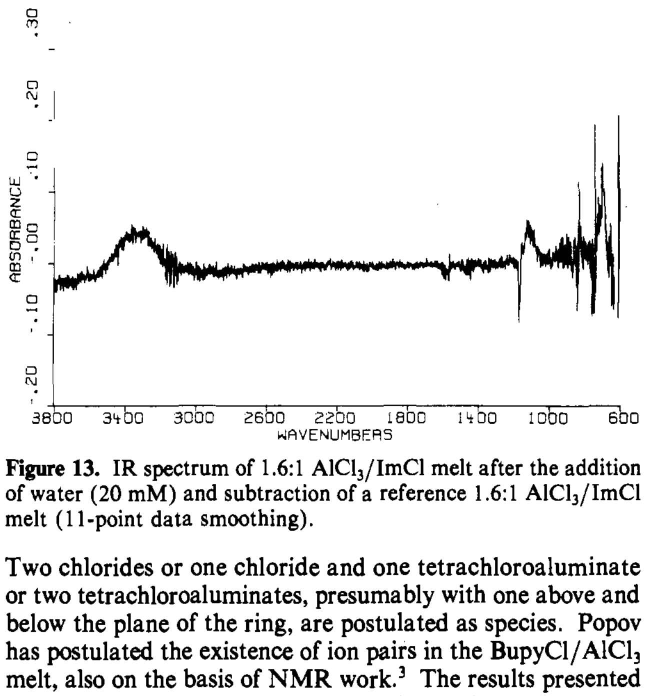

Figure 13. IR spectrum of 1.6:1 $AlCl_3$/ImCl melt after the addition of water (20 mM) and subtraction of a reference 1.6:1 $AlCl_3$/ImCl melt (11-point data smoothing).

Two chlorides or one chloride and one tetrachloroaluminate or two tetrachloroaluminates, presumably with one above and below the plane of the ring, are postulated as species. Popov has postulated the existence of ion pairs in the BupyCl/$AlCl_3$ melt, also on the basis of NMR work.[3] The results presented above, particularly with regard to the isosbestic point appearance and variation with acidity, appear to lend support to a two-species—i.e., ion-pair—interaction. It is possible that whatever specific interaction takes place giving rise to the isosbestic point(s) depends only on whether or not the closest neighbor to the imidazolium ring is a single chloride ion; the formation of an oligomer by some time-averaged proximity of a second chloride to the initial Bupy$^+$/Im$^+$Cl$^-$ "ion pair" may not result in additional perturbations sufficient to result in further IR spectral changes.

The frequency at 703 cm^{-1} could not be assigned to a cation vibration (unless it is the aliphatic C–H bending mode, which is unlikely[13]), and it increased in size without any change in peak frequency as the melt acidity was increased. Since Al–O stretching bands are known to exist in this region,[23,24] the possibility that this was linked to the "aging" of melts was examined by adding water.

Addition of Water to ImCl/$AlCl_3$ Melts. 1.6:1 $AlCl_3$/ImCl Acid Melt. Acidic melts react with water in a highly exothermic manner with the evolution of hydrogen chloride and the formation of a white precipitate. This redissolves on stirring, and the spectrum of this melt (20 mM water) after subtraction of a reference 1.6:1 $AlCl_3$/ImCl melt spectrum

---

(21) Leonard, N.; Gash, V. *J. Am. Chem. Soc.* **1954**, *76*, 2781.

(22) Leonard, N.; Thomas, P.; Gash, V. *J. Am. Chem. Soc.* **1955**, *77*, 1552.

(23) Nakamoto, K. "IR and Raman Spectra of Inorganic and Coordination Compounds"; Wiley Interscience: New York, 1978.

(24) Moolenaar, R.; Evans, J.; McKeever, L. *J. Phys. Chem.* **1970**, *74*, 3629.

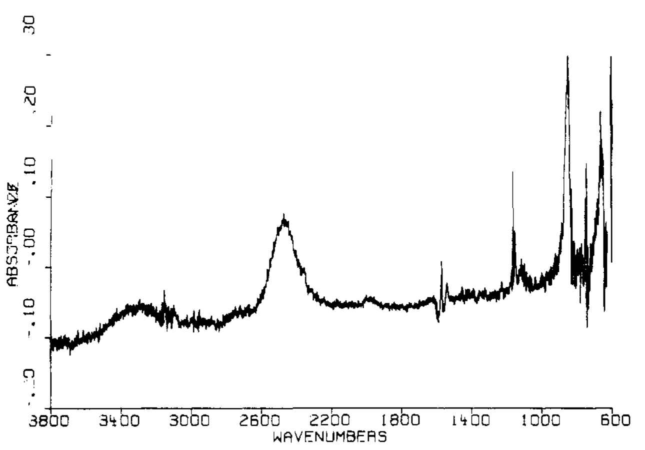

Figure 14. IR spectrum of a 1.6:1 $AlCl_3$/ImCl melt after the addition of D_2O (60 mM) and subtraction of a reference 1.6:1 $AlCl_3$/ImCl melt (11-point data smoothing).

Table VI. Comparison of the IR Peak Frequencies (cm^{-1}) of Aluminoxy Species

compd	peak freq[a]	source
$(Al_2(H_2O)_8OH_2)^{4+}$	3520, 3300, 3130, 2500, 1950, 1080, 980, 790, 730, 630	ref 24
H_2O	3490, 1650, 700	ref 24
$Al(OH)_3$	3480, 1620, 1010, 760, 530	Sadtler Index Y18K
Al_2O_3	700, 450	Sadtler Index Y175K
1.6:1 $AlCl_3$/ImCl + H_2O	3323, 1118, 703	this work
1.6:1 $AlCl_3$/ImCl + D_2O	2477 (0.75), 853 (0.76), 662 (0.94)	this work
0.4:1 $AlCl_3$/ImCl + H_2O	3520, 3360, 3100, 2410, 2170, 2050, 1170, 1180	this work
0.4:1 $AlCl_3$/ImCl + D_2O	2423 (0.72), 2265 (0.73)	this work

[a] Figures in parentheses are the ratio of the peak frequency in H_2O to the frequency in D_2O.

is shown in Figure 13. The same spectrum for the addition of D_2O is shown in Figure 14. The peak frequencies are compared in Table VI with other aluminoxy species.

The subtracted spectrum only contains three bands at 3323, 1119, and 703 cm^{-1}, which increase linearly in magnitude with further additions of water. Both the 3323- and 1119-cm^{-1} bands disappeared with D_2O was added (60 mM) (apart from some traces of water in the D_2O), and new bands were found at 2477 and 853 cm^{-1}. The ratio of the two bands in each case was close to the theoretical shift of 0.76, and the bands were assigned to O–H stretching and O–H bending, respectively. These bends are typical for an inorganic compound containing a hydroxy group.[23] The 703-cm^{-1} band shifts by only a factor of 0.94 and was assigned to an Al–O–H stretching mode. A similar band is found in the spectra of aluminum oxide, aluminum hydroxide (see Table VI), and chloroaluminoxy species,[24–26] though studies on the latter were obtained in aqueous media where the coordination of water and the formation of dimers complicate the spectrum. The absence of any Al–O–Al absorbances, which typically occur near 2400 cm^{-1} (e.g., as in aluminum oxide), indicates that dimers are not formed in the acidic melt.[25] Since the spectrum shows no dimers, the initially insoluble material must be dissolving as a monomeric species such as AlO(OH), $Al(OH)Cl_2$, or $Al(OH)_2Cl$.

A study by Moolenaar et al.[24] showed that a dihydroxy anion $AlO(OH)_2^-$ has absorbances at 900, 705, and 540 cm^{-1}. By analogy, $Al(OH)_2Cl$ becomes unlikely as only one of the two possible bands visible in the transmission range is observed. Differentiating between AlO(OH) and $Al(OH)Cl_2$ is difficult as the IR region below 600 cm^{-1} is obscured by melt and window absorbances that prevent a search for the presence of Al–Cl stretching or dihydroxy antisymmetric bending modes. Of the two species, $AlOHCl_2$ is the more probable as the hydrogen atom on AlO(OH) would be shared, leading to shifted peak frequencies and broader bands. In addition, previous electrochemical studies[1,27] suggested that AlOCl was the aluminoxy species arising in acid melt when oxide was added, and $Al(OH)Cl_2$ is closer to this than AlO(OH).

Further additions of water to the melt led to the emergence of other bands in the spectrum (a broad multipeaked band centered at 2175 cm^{-1} and another at 1230 cm^{-1}), possibly indicating the presence of other species at higher concentrations of added water.

0.4:1 $AlCl_3$/ImCl Melt. Water (60 mM) reacted slowly with the basic melt to give a white precipitate that redissolved on stirring. (Not all of this precipitate redissolved when water was added to an approximately neutral melt.) The IR spectrum of the melt and redissolved precipitate after subtraction of a reference 0.4:1 $AlCl_3$/ImCl melt was complex but showed similarities with spectra obtained by Riesgraf and May,[26] who added freshly prepared aluminum hydroxide gels to aluminum chloride solutions. At least three bands were observed in the O–H stretching region (3520 (?), 3350, 3100 cm^{-1}) and two in the O–H bending region (1180, 1190 cm^{-1}). The remaining bands in the spectrum are weak and/or broad, though similarities exist between this spectrum and that of Riesgraf and May.[26] On addition of D_2O (60 mM), the bands assigned to the hydroxy group all shifted to lower frequencies by a factor close to 0.76 as before.

Recent work suggested that water reacts to form HCl and some unknown aluminum hydroxy species.[28]

The formation of an Al–OH species in the chloroaluminate melt explains some of the results obtained during an electrochemical study of oxide and water addition in a basic BupyCl/$AlCl_3$ melt in the presence of Ti(IV).[1] Two Ti(IV) reduction waves were found, which varied with oxide concentration as a result of the equilibria

$$O^{2-} + AlCl_4^- \rightleftarrows AlOCl_2^- + 2Cl^-$$

$$TiCl_6^{2-} + AlOCl_2^- \rightleftarrows TiOCl_4^{2-} + AlCl_4^-$$

the latter equilibrium being quite slow. The addition of water shifted the Ti(IV) equilibrium to the left, indicating that water acted to remove $AlOCl_2^-$. The formation of an Al–OH–Cl species would account for the observed chemistry.

Acknowledgment. Discussions with T. Zawodzinski, Drs. Zenon Karpinski, Saeed Sahami, M. Lipsztajn, and J. O'Dea contributed to this work as did discussions with Dr. John Wilkes, Frank J. Seiler Laboratory of the U.S. Air Force Academy, and with Professor C. D. Ritchie. This work was supported in part by the Office of Naval Research.

Registry No. BupyCl, 1124-64-7; ImCl, 65039-09-0; $AlCl_3$, 7446-70-0; AlO(OH), 24623-77-6; $AlOHCl_2$, 14215-15-7; H_2O, 7732-18-5; D_2O, 7789-20-0.

---

(25) McIntyre, J.; Foley, R.; Brown, B. *J. Appl. Spectrosc.* **1982**, *36* (2), 128.

(26) Riesgraf, D.; May, M. *J. Appl. Spectrosc.* **1978**, *32* (4), 362.

(27) Tremillon, B.; Bermond, A.; Molina, R. *J. Electroanal. Chem. Interfacial Electrochem.* **1976**, *74*, 53.

(28) Sahami, S.; Osteryoung, R. A. *Anal. Chem.* **1983**, *55*, 1970.